1990   Journal Article

Chemiluminescent Reactions of Group VI Atoms (O(^{3}P) and Se(^{3}P)) with Azide Radicals

2301-F1-74

Andrew P. Ongstad, Thomas L. Henshaw,
Robert I. Lawconnell, William G. Thorpe

F. J. Seiler Research Laboratory
USAF Academy CO 80840-6528

FJSRL-JR-90-0015

The O(^{3}P) + N$_3$($^2\Pi_g$) $\rightarrow$ NO + N$_2$ and Se(^{3}P) + N$_3$($^2\Pi_g$) $\rightarrow$ NSe + N$_2$ chemiluminescent reactions have been studied in a conventional discharge flow reactor using chemiluminescence detection of NO(A$^2\Sigma^+$) and atomic resonance fluorescence detection of Se(^{3}P) to follow the rate of the reactions. The O + N$_3$ reaction produces electronically excited NO(A$^2\Sigma^+$) in a nonthermal vibrational distribution of v(0): 0.64, v(1): 0.31, and v(2): 0.05. The high energy limit serves to place bounds on the heat of formation of N$_3$ indicating $107.8 > \Delta H_f \geq 101.3$ kcal mol^{-1}. The NO(A $\rightarrow$ X) photon yield and rate coefficient for the reaction were determined to be $\phi_{A \rightarrow X}^{NO} = 0.3\%$ and $k_1 = (1.12 \pm .18) \times 10^{-11}$ cm^3 s^{-1}, respectively. The rate of the O(^{3}P) + HN$_3$ $\rightarrow$ OH + N$_3$ reaction was also measured and found to be slow with $k_9 \leq 2 \times 10^{-13}$ cm^3 s^{-1}. The Se + N$_3$ reaction produces electronically excited NSe (A$^2\Pi_{1/2 \ 3/2}$) with a rate coefficient of $(6.4 \pm 2.4) \times 10^{-12}$ cm^3 s^{-1}. The photon yield for this reaction is also small: $\phi_{A \rightarrow X}^{NSe} = 0.02\%$. The low yields of the excited products in the Group VI plus N$_3$ reactions are viewed in terms of weak angular orbital momentum constraints and a large number of reactant surfaces.

Nitrogen ozides Chemiluminescence Azides	15. NUMBER OF PAGES 7
	16. PRICE CODE

17. SECURITY CLASSIFICATION OF REPORT	18. SECURITY CLASSIFICATION OF THIS PAGE	19. SECURITY CLASSIFICATION OF ABSTRACT	20. LIMITATION OF ABSTRACT
UNCLASSIFIED	UNCLASSIFIED	UNCLASSIFIED	NONE

Chemiluminescent Reactions of Group VI Atoms (O(^{3}P) and Se(^{3}P)) with Azide Radicals

Andrew P. Ongstad,* Thomas L. Henshaw, Robert I. Lawconnell, and William G. Thorpe

Frank J. Seiler Research Laboratory, USAF Academy, Colorado 80840-6528 (Received: December 27, 1989; In Final Form: March 14, 1990)

The O(^{3}P) + N$_3$($^2\Pi_g$) → NO + N$_2$ and Se(^{3}P) + N$_3$($^2\Pi_g$) → NSe + N$_2$ chemiluminescent reactions have been studied in a conventional discharge flow reactor by using chemiluminescence detection of NO(A$^2\Sigma^+$) and atomic resonance fluorescence detection of Se(^{3}P) to follow the rate of the reactions. The O + N$_3$ reaction produces electronically excited NO(A$^2\Sigma^+$) in a nonthermal vibrational distribution of $v(0)$ 0.64, $v(1)$ 0.31, and $v(2)$ 0.05. The high-energy limit serves to place bounds on the heat of formation of N$_3$ indicating $107.8 > \Delta H_f \geq 101.3$ kcal mol^{-1}. The NO(A→X) photon yield and rate coefficient for the reaction were determined to be ϕ_{A-X}^{NO} = 0.3% and $k_1 = (1.12 \pm 0.18) \times 10^{-11}$ cm^3 s^{-1}, respectively. The rate of the O(^{3}P) + HN$_3$ → OH + N$_3$ reaction was also measured and found to be slow with $k_9 \leq 2 \times 10^{-13}$ cm^3 s^{-1}. The Se + N$_3$ reaction produces electronically excited NSe (A$^2\Pi_{1/2,3/2}$) with a rate coefficient of $(6.4 \pm 2.4) \times 10^{-12}$ cm^3 s^{-1}. The photon yield for this reaction is also small: ϕ_{A-X}^{NSe} = 0.02%. The low yields of the excited products in the group VI plus N$_3$ reactions are viewed in terms of weak angular orbital momentum constraints, a large number of reactant surfaces, and the potential for disposing a large fraction of the reaction exothermicity to ground-state products.

Introduction

Much recent work has been done on the chemiluminescent reactions of atomic species (R) with azide radicals (N$_3$).[1] These reactions typically produce excited-state nitrides or nitrenes which subsequently emit in the UV and visible regions. The high product specificity and large quantum yields observed in many of these reactions has been attributed to electron spin[2] and/or orbital angular momentum constraints.[3] Spin constraints have been found to be important in reactions of the group VII (halogens) atoms, and orbital constraints have been found to play a role in group V atom reactions. Since N$_3$ may be regarded as an excited N(^{2}D) atom loosely bound to N$_2$(X), the extent to which orbital correlations are important depends upon the degree to which the reactive nitrogen of N$_3$ retains ^{2}D character along the reaction coordinate; i.e., the NR product should correlate to N(^{2}D) + R. Reactions of group VI atoms with N$_3$ have received less attention even though they are also of interest as chemiluminescent reactions capable of producing specific electronic states of group VI nitrides. The reactions of group VI atoms with N$_3$

$$\text{O}(^3\text{P}) + \text{N}_3(^2\Pi) \rightarrow \text{N}_2 + \text{NO} \quad -137 \text{ kcal mol}^{-1} \quad (1)$$

$$\text{S}(^3\text{P}) + \text{N}_3(^2\Pi) \rightarrow \text{N}_2 + \text{NS} \quad -102 \text{ kcal mol}^{-1} \quad (2)$$

$$\text{Se}(^3\text{P}) + \text{N}_3(^2\Pi) \rightarrow \text{N}_2 + \text{NSe} \quad -77 \text{ kcal mol}^{-1} \quad (3)$$

are sufficiently energetic to populate a number of electronic states of NO, NS, and NSe. As explained above, the degree of conservation of orbital angular momentum is defined by the correlation of the NR product to N(^{2}D) + R(^{3}P); i.e., the B$^2\Pi$ excited states of NO and NS and the A$^2\Pi$ state of NSe. The early studies on the O + N$_3$ reaction[4,5] have indicated that the NO(B$^2\Pi$) state is not observed in reaction 1, which produced NO(A$^2\Sigma^+$) exclusively from several energetically allowed states. Further, our recent investigation of the S + N$_3$ reaction[6] has shown that even though NS β-band emission (B$^2\Pi$ → X$^2\Pi$) is readily observed, the NS-
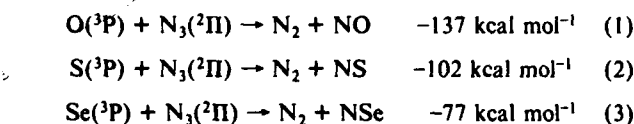
(B$^2\Pi$) state is produced in very low yield. These results appear to indicate that, in marked contrast to the group V atom plus azide reactions, the orbital angular momentum correlations are much weaker for the group VI atom reactions and that these reactions may dispose a large fraction of their energy into the ground and other dark states.

In this paper we have extended our studies of the group VI azide reactions to include the reactions of O(^{3}P) and Se(^{3}P) atoms with N$_3$, reporting measurements of the rate coefficients for the reactions 1 and 3 and spectroscopic observations on the chemiluminescence generated. The spectroscopic data is compared with earlier work and the overall trends in reactions of group VI atoms are examined. The strengths of the angular momentum correlations are compared to those of other azide reactions. The data are of interest with respect to a possible chemically or optically pumped laser since the excited group VI nitride diatomics have features which make them attractive laser candidates. Burrows and co-workers have already demonstrated an optically pumped NO(A→X) laser.[7]

Experimental Section

The experimental apparatus has been described in detail elsewhere.[6] The experiments utilized a conventional discharge flow reactor with chemiluminescence or resonance fluorescence detection. The 50 cm long flow reactor was fabricated from 2.54 cm i.d. Pyrex tubing and had two side arms equipped with 2450-MHz microwave discharge cavities for atom production. Fluorine atoms were produced by a discharge through carrier gas/CF$_4$ or carrier gas/F$_2$. Nitrogen atoms were generated by passage of carrier gas/N$_2$ mixtures through the discharge. F and N atom number densities were determined by chemiluminescent titrations.[8,9] To reduce F atom wall reactions, the flow tube was coated with halocarbon wax.

The flow tube contained a sliding injector for temporal resolution. Two different injectors were used. In the investigation of the O + N$_3$ and the O + HN$_3$ reactions, the injector was equipped with a microwave discharge cavity to provide for the production of oxygen atoms. To reduce background emissions emanating from the discharge of dilute He/O$_2$ mixtures, the cavity was positioned off the flow tube axis on a side arm assembly which contained a Woods Horn light trap. In measurements of the rate coefficient for the O + HN$_3$ reaction, oxygen atoms were detected

(1) (a) May, D. J.; Coombe, R. D. *J. Phys. Chem.* **1989**, *93*, 520. (b) Henshaw, T. L.; McElwee, D.; Stedman, D. H.; Coombe, R. D. *J. Phys. Chem.* **1988**, *92*, 4606. (c) Ongstad, A. P.; Coombe, R. D.; Neumann, D. K.; Stech, D. J. *J. Phys. Chem.* **1989**, *93*, 549.

(2) Pritt, A. T.; Patel, D.; Coombe, R. D. *Int. J. Chem. Kinet.* **1984**, *16*, 977.

(3) (a) Henshaw, T. L.; MacDonald, M. A.; Stedman, D. H.; Coombe, R. D. *J. Phys. Chem.* **1987**, *91*, 2838. (b) David, S. J.; Coombe, R. D. *J. Phys. Chem.* **1985**, *89*, 5206.

(4) Clark, T. C.; Clyne, M. A. A. *Trans. Faraday Soc.* **1970**, *66*, 877.

(5) Piper, L. G.; Krech, R. H.; Taylor, R. L. *J. Chem. Phys.* **1979**, *71*, 2099.

(6) Henshaw, T. L.; Ongstad, A. P.; Lawconnell, R. I. *J. Phys. Chem.* **1990**, *94*, 3602.

(7) Burrows, M. D.; Baughcum, S. L.; Oldenborg, R. C. *Appl. Phys. Lett.* **1985**, *46*, 22.

(8) Ganguli, P. S.; Kaufman, M. *Chem. Phys. Lett.* **1974**, *25*, 221.

(9) See, for example: Clyne, M. A. A. In *The Physical Chemistry of Fast Reactions*; Levitt, B. P., Ed.; Plenum Press: London, 1973; Chapter 4.
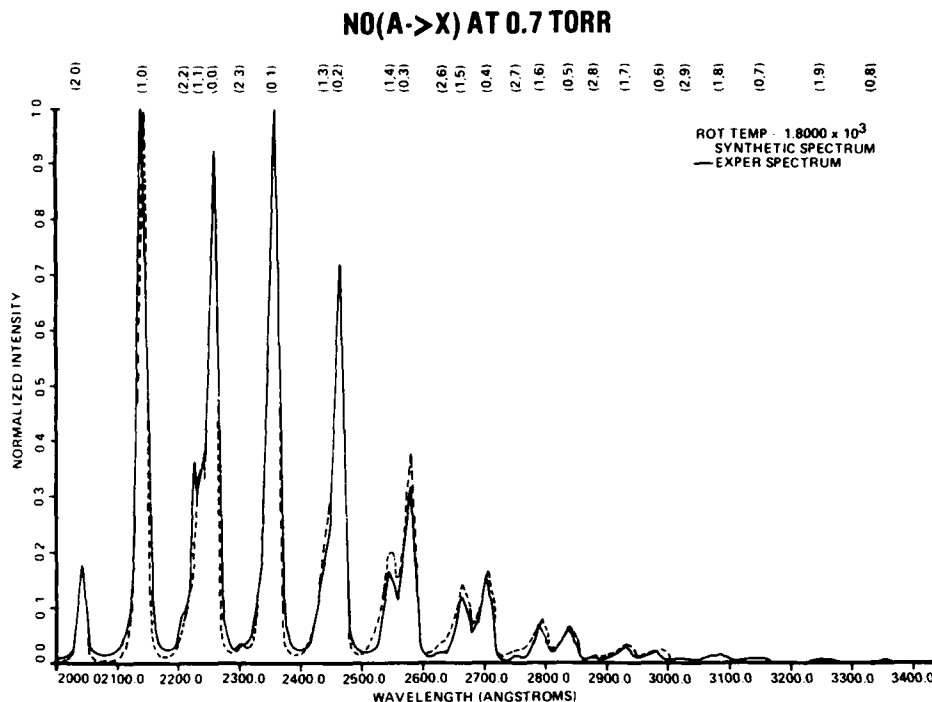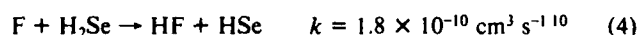
NO(A->X) AT 0.7 TORR

Figure 1. Chemiluminescent spectrum of NO($A^2\Sigma^+$) produced by the O/F/HN$_3$ system. The dashed line is a simulated spectrum using the experimentally determined vibrational populations (N_v). From line-width analysis of the synthetic spectrum, a rotational temperature of 1800 ± 600 K was obtained.

by their chemiluminescent reaction with NO, which was added through a titration port near the detection volume. Oxygen atom densities were determined by titration with NO$_2$. A dual concentric injector was employed in the investigation of the Se + N$_3$ reaction. Dilue flows of H$_2$Se entered the flow reactor via the outermost tube of the double injector. Ground-state Se atoms were then generated by the reaction of F atoms with H$_2$Se:

$$F + H_2Se \rightarrow HF + HSe \qquad k = 1.8 \times 10^{-10} \text{ cm}^3 \text{ s}^{-1} \text{ [10]} \qquad (4)$$

$$F + HSe \rightarrow HF + Se \qquad (5)$$

The rate constant for reaction 5 has not been reported, but on the basis of similar H-atom abstraction reactions[10] (e.g., F + HS → HF + S, $k = 5 \times 10^{-10}$ cm^3 s^{-1}), it is expected to be large. Azide radicals were produced by the reaction of F atoms with HN$_3$. In the studies of reactions 1 and 3, the HN$_3$ entered the flow reactor either through the side arm across from the F atoms discharge or through the centermost injector, respectively.

The system was pumped by a Kinney KT-300 mechanical pump whose free-air displacement is 142 L/s. To ensure adequate mixing, the pump was throttled to produce linear flow velocities in the range 11–25 m/s with pressure of 0.7–2.0 Torr. Flows of gases into the flow reactor were measured by calibrated mass flow meters (Matheson Model 8102) and pressures were measured with a calibrated capacitance manometer (MKS Baratron). The pressure port was located a few centimeters above the resonance fluorescence detection cell.

The flow tube was coupled to a chemiluminescence/resonance fluorescence detection cell fabricated from a 10 cm^2 × 10 cm aluminum block. The cell was equipped with two 1-in. MgF$_2$ windows and a resonance lamp constructed from 12 mm o.d. quartz tubing and fitted with a microwave discharge cavity. The windows and resonance lamp were positioned at right angles to the flow reactor. To reduce scattered light, the cell was also equipped with a Woods Horn (on axis with the flow tube) and was anodized black. Dilute flows of 0.5% H$_2$Se discharged in the resonance lamp produced Se resonance lines at 196.03, 203.98, 206.28, and 207.48 nm. The 207.48-nm line was used as the excitation wavelength since its intensity was largest.

(10) Agrawalla, B. S.; Setser, D. W. *J. Phys. Chem.* **1986**, *90*, 2450.

Emissions from electronically excited atoms and molecules were dispersed with a 0.25-m polychromator and detected with a 1024-element silicon diode array. Data acquisition and storage was performed with a PAR Model 1460 OMA III system. Calibration of the system's spectral sensitivity was performed with an Optronics Laboratory deuterium lamp and standard lamp. Alternatively, for spectral analysis requiring greater sensitivity and higher resolution, emissions were dispersed with a 0.3-m monochromator and detected with a cooled GaAs photomultiplier tube (PMT) (RCA C31034A).

Hydrazoic acid was synthesized by reacting stearic acid with NaN$_3$ at 115 °C under vacuum. The gas was collected in 12-L glass bulbs and diluted with ultra-high-purity (UHP) He to obtain mixtures near 3% reactant concentration. Commercially obtained helium (UHP), O$_2$ (UHP), N$_2$ (UHP), F$_2$ (5% in He), CF$_4$ (99.95%), Cl$_2$ (10% in He), NO (99%), NO$_2$ (99.5%), and H$_2$Se (98%) were used without further purification. However, during the course of the experiments it became evident that NO(A→X) (γ bands) background emission needed to be reduced such that it would not complicate the study of reaction 1. To this end a gas purifier (oxyclear) was installed in the He carrier gas line and, further, the He and F$_2$/He flows were passed through liquid nitrogen cold traps. These measures reduced the NO(A→X) emission to extremely low levels.

Results

1a. Spectroscopy of the O/F/HN$_3$ Flame. The addition of small flows of HN$_3$ to a stream containing F and O atoms, heavily diluted in He, gave rise to the spectrum shown in Figure 1. The spectrum is attributable to the $v' = 0$, 1, and 2 progressions from the $A^2\Sigma^+ \rightarrow X^2\Pi$ transition in NO. No evidence for emission from higher A state vibrational levels (i.e., $v' > 2$), or from other electronically excited states of NO, namely B$^2\Pi \rightarrow$ X$^2\Pi$ emission, was obtained. The dependence of the NO(A) band system was checked as a function of reagent flows and was found to be strongly dependent on the CF$_4$ or F$_2$, HN$_3$, and O$_2$ flow rates. Removal of any of these reagents markedly reduced the γ-band emissions. However, when either the CF$_4$ (or F$_2$) or the O$_2$ flow was removed, a small background emission remained. This background was typically ≤5% of the original intensity.

In these experiments, the typical starting F atom and HN$_3$ densities were ≤1 × 10^{13} atoms cm^{-3} and 3 × 10^{13} molecules cm^{-3},

WAVELENGTH (nm)
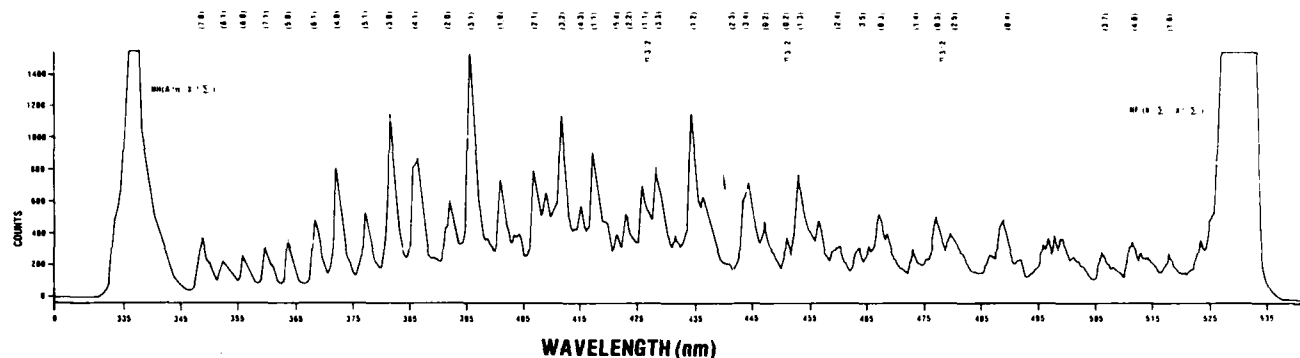
Figure 2. Chemiluminescent spectrum of NSe($A^2\Pi_{1/2,3/2}$) produced by the $H_2Se/F/HN_3$ system. The transitions assigned to NSe($A_2{\rightarrow}X_2$), NH-($A^3\Pi{\rightarrow}X^3\Sigma^-$), and NF($b^1\Sigma^+{\rightarrow}X^3\Sigma^-$) are indicated.

respectively. These reagents were introduced collinearly into the flow tube from 10 to 50 cm upstream of the central injector. This allowed for the conversion of F to HF and N_3 radicals by the rapid reaction.[11]

$$F + HN_3 \rightarrow HF(v) + N_3 \qquad k = 1.8 \times 10^{-10} \text{ cm}^3 \text{ s}^{-1} \qquad (6)$$
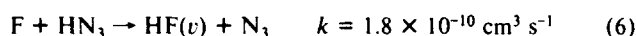
Since several milliseconds were allowed for the reaction and large densities of HN_3 were used, the N_3 was generated in less than 1 ms (1 ms $\sim 5\tau$) and the starting F atom density gave the initial N_3 density. The initial O atom densities were typically $\leq 5 \times 10^{13}$ atoms cm^{-3}.

A long-lived green flame became apparent at higher F atom flow rates. This emission corresponded to the $v' = 0$ sequence of the $b^1\Sigma^+ \rightarrow X^3\Sigma^-$ transition of NF. At the nominally low flows of F used in these experiments the NF emission was not visible to the eye but still electronically detectable via the monochromator and PMT. The integrated NF(b) intensity was typically several orders of magnitude less than the NO(A) intensity. NF(b) is known to be formed by an energy pooling reaction between HF-(v+2) and NF(a) where the NF(a) is formed by a secondary reaction.[2,11]

$$F + N_3 \rightarrow NF(a^1\Delta) + N_2 \qquad k = 1.8 \times 10^{-12} \text{ cm}^3 \text{ s}^{-1} \qquad (7)$$

A narrow spectral feature was also observed at 336 nm and corresponded to the $A^3\Pi_i \rightarrow X^3\Sigma^-$ transition in NH. Its relative intensity was also much weaker than that from NO(A). The origin of the NH(A) in the flow reactor most likely arises from collisions between $N_2(A^3\Sigma_u^+)$ and HN_3.[12]

$$N_2(A) + HN_3 \rightarrow NH(A) + 2N_2 \qquad (8)$$

where the production of triplet N_2 metastables is thought to occur from surface decomposition of N_3 radicals or from N_3 disproportionation.[11] The quenching of $N_2(A)$ by HN_3 has a reported rate constant[13,14] in the range (7–8) $\times 10^{-11}$ cm^3 s^{-1} with a branching fraction of 3% to the A state.[14] Given the relatively high densities of HN_3 in the flow reactor, any $N_2(A)$ produced would be rapidly quenched and, as such, it is unlikely that energy transfer between $N_2(A)$ and NO to produce NO(A), known to be a relatively facile process, could account for the observed NO emission. However, to test this supposition, an experiment was performed to gauge $N_2(A)$ densities in the reactor. In the experiment, the O_2 discharge was inactivated and a small flow of NO added through the injector. The NO density was high enough (approximately 10^{12} molecules cm^{-3}) to observe potentially strong NO(A) emission but not so large as to produce significant NO–NO(A) self-quenching. No increase in NO emission over background levels was observed, indicating low $N_2(A)$ densities in the reactor.

No other emissions were observed at wavelengths beyond 340 nm (aside from NF(b), mentioned above). Specifically, no emission from NF(a) and no nitrogen first positive or any air

afterglow emission from the O + NO recombination reaction was apparent.

1b. Spectroscopy of the $F/H_2Se/HN_3$ Flame. When a dilute flow of $H_2Se(\leq 2 \times 10^{12})$ was added to a flow of fluorine atoms ($\leq 5 \times 10^{14}$ atoms cm^{-3}), Se atoms were generated by reactions 4 and 5. To ensure adequate conversion of H_2Se to Se, several centimeters of reaction time were allowed prior to the introduction of HN_3 in the flow reactor. Measurements of the Se atom production via atomic resonance fluorescence indicated the reaction time was long enough for efficient conversion of H_2Se to Se atoms. As above, azide radicals were generated by the F + HN_3 reaction at concentrations of $\leq 2 \times 10^{14}$ molecules cm^{-3}.

The addition of HN_3 to a stream of F and Se atoms created a flame visually distinct in two regions: a short violet chemiluminescent flame followed by a much longer lived diffuse blue afterglow. The spectrum of the violet portion of the flame is shown in Figure 2 and is primarily attributable to the $A_1 \rightarrow X_1$ transition of NSe (T_e = 24 350 cm^{-1}).[15,16] Bands from the $A_2 \rightarrow X_2$ transition, which lie slightly lower in energy (T_e = 24 800 cm^{-1}), are also apparent, although only emission from the $v' = 0$ and $v' = 1$ levels are observed. The spectrum displays a small Franck–Condon shift with the (3,1) band being the most intense out of the $v' = 3$ progression. The spectrum is strongly overlapped by NH($A{\rightarrow}X$) and NF($b{\rightarrow}X$) emission. Nitrogen first positive emission (B $\rightarrow$ A) and NF(a $\rightarrow$ X) were also detected at longer wavelengths. The origin of the NF and NH chemiluminescence is most likely due to reactions 7 and 8, respectively, as explained above. The intensity of the NSe($A_1{\rightarrow}X_1$) emission was found to be strongly dependent on the CF_4, H_2Se, and HN_3 flows. Removal of any of these reagents caused the cessation of NSe-($A{\rightarrow}X$) fluorescence. The role of the nitrogen metastables was again examined by adding small flows of NO to the reactive stream. As expected, the addition of NO effectively quenched the $N_2(B{\rightarrow}A)$ emission and a concomitant increase in the NO(γ) bands was observed. At the maximum NO(A) density, corresponding to a density of 3 $\times 10^{13}$ molecules cm^{-3} of added NO(X), the NH(A) band was quenched by 60%. In contrast, the NSe bands were only reduced by 33%. Further, the NSe(A_1) vibrational distribution was not significantly altered by the addition of NO.

Spectral analysis of the long-lived blue portion of the flame revealed a continuum emission extending from 380 to 510 nm. The continuum was strongly dependent on the flows of CF_4, HN_3, and H_2Se. The luminescence was also quenched by the addition of small flows of NO.

The Se atoms and N_3 generated in the system may undergo a bimolecular reaction to produce NSe:

$$Se(^3P) + N_3(^2\Pi) \rightarrow NSe + N_2(X) \qquad (3)$$

The enthalpy change of the reaction can be calculated from standard heats of formation.[17] Taking ΔH_f(NSe) = 69.16 kcal

(11) David, S. J.; Coombe, R. D. *J. Phys. Chem.* **1986**, *90*, 3260.
(12) Stedman, D. H.; Setser, D. W. *Chem. Phys. Lett.* **1968**, *2*, 542.
(13) Coombe, R. D.; David, S. J.; Henshaw, T. L.; May, D. J. *Chem. Phys. Lett.* **1985**, *120*, 433.
(14) Cao, D. F.; Setser, D. W. *J. Phys. Chem.* **1988**, *92*, 1169.

(15) Daumont, D.; Jenouvrier, A.; Pascat, B. *Can. J. Phys.* **1976**, *54*, 1292.
(16) Huber, K. P.; Herzberg, G. *Molecular Spectra and Molecular Structure IV Constants of Diatomic Molecules*; Van Nostrand: New York, 1970.
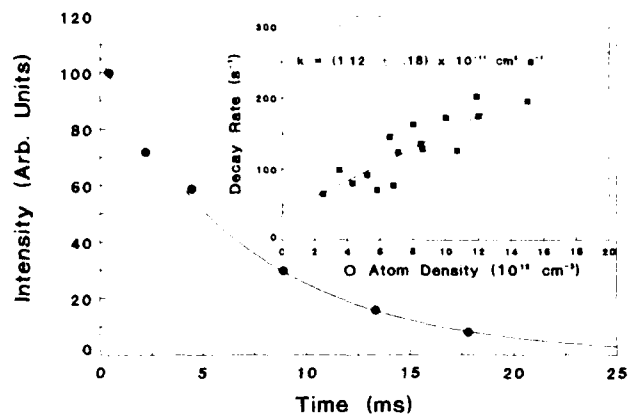
Figure 3. Typical time profile of the γ-band emission, (0,1) band. The initial densities of O, F, and HN_3 were 8.5×10^{12}, 4×10^{11}, and 1×10^{13} molecules cm^{-3}, respectively. The closed circles are the individual data points and the line represents a nonlinear least squares fit to a function $I = ce^{-\gamma t}$. A plot of the pseudo-first-order decay rate vs O-atom density is shown in upper right-hand corner. The slope of the line gives the second-order rate constant for the O + N_3 reaction.

Figure 4. Time profile of the Se atomic resonance fluorescence emission near 204 nm. The densities of F, H_2Se, and HN_3 were 5×10^{13}, 1.6×10^{12}, and 1.4×10^{13} molecules cm^{-3}, respectively. The closed circles are the individual data points and the line is a nonlinear least-squares fit to the data. The inset figure shows a plot of the pseudo-first-order decay rate against N_3 density. The least-squares slope gives the Se + N_3 bimolecular rate constant.

mol^{-1}, $\Delta H_f(Se) = 48.4$ kcal mol^{-1} (where the dissociation energy of NSe^{16} has been used to calculate its heat of formation), and $\Delta H_f(N_3) = 99.1$ kcal mol^{-1}, the exothermicity of the reaction is calculated to be -78.3 kcal mol^{-1}. This represents enough energy to populate the A_1 state of NSe up to $v' = 4$. However, we have confirmed levels populated up to at least $v' = 8$. The discrepancy may be due to the uncertainties in the heat of formation of N_3. Habdas et al.[18] reported a substantially larger value for the ΔH_f of N_3 of 113 kcal mol^{-1}. Using this value, we calculate a thermodynamic limit of -92.2 kcal mol^{-1} for reaction 3. This represents enough energy to populate the A_1 state to $v' = 12$. However, population of $NSe(A_1)$ above $v' = 8$ could not be confirmed due to the presence of $NH(A \rightarrow X)$ and NO γ-band emission in this spectral region.

Two quartet states, the a $^4\Pi_i$ and b $^4\Sigma_{1/2}^-$, are believed to lie in close proximity to the A_1 and A_2 states. In a high-resolution study[15] of the $^{15}N^{80}Se$ spectrum in the 330–580-nm region, Daumont, Jenouvrier, and Pascat have detected the presence of these close-lying states mainly through perturbations on the ro-vibrational manifold of the A states. In addition, they have also identified a weak transition thought to originate from the b $^4\Sigma^-$ state. The resolution of the present experiments was not high enough to detect possible interaction from these quartet states.

2a. Kinetics of the O + N_3 and O + HN_3 Reactions. Time profiles of the NO(A) emission were measured by movement of the sliding injector (the O atom source) with respect to the fixed observation zone. A typical time profile recorded for the (0,1) band near 237.0 nm is shown in Figure 3 and is well fit by an exponential function. The decays were measured under pseudo-first-order conditions with O atoms in large excess over N_3 radicals. Since reaction 6 was used to produce the N_3 radicals, the starting F atom densities ($\leq 4 \times 10^{11}$) gave the initial N_3 densities. O and F atom concentrations were determined by titration with NO_2 and Cl_2, respectively.[8,19] The lifetimes of the decays varied inversely with the O atom concentration and this behavior is identified with the rate of formation of NO(A) by the O + N_3 reaction. The rate coefficient for the reaction was determined by plotting the pseudo-first-order decay rate against the O atom density. The slope of the plot, shown in Figure 3, gives the rate constant $k = (1.12 \pm 0.18) \times 10^{-11}$ cm^3 s^{-1}, where the error reflects the scatter in the data. This value is in good agreement with that reported by Piper, Krech, and Taylor.[4] In their study of the thermal decomposition of NaN_3, they determined a less precise value of $(1 \pm 0.4) \times 10^{-11}$ cm^3 s^{-1}.

The nonzero intercept indicates the occurrence of N_3 wall reactions. The N_3 wall removal rate of 39 ± 15 s^{-1} is similar to the value reported by David and Coombe[11] who measured $k_w = 46 \pm 0.04$ s^{-1} for a 3.5 cm i.d. PTFE flow reactor.

A series of rate measurements were performed to determine the importance of the reaction

$$O + HN_3 \rightarrow OH + N_3 \qquad \Delta H_0 = -22.2 \text{ kcal mol}^{-1} \qquad (9)$$

in the $O/F/HN_3$ chemical system. O atoms were detected[19,20] by the chemiluminescent reaction that occurred when NO (3.2×10^{15} molecules cm^{-3}) was added through a titration port slightly upstream of the detection volume:

$$O + NO \rightarrow NO_2^* \qquad (10)$$

$$NO_2^* \rightarrow NO_2 + h\nu \qquad (11)$$

The green-yellow "air afterglow" was detected by an RCA C31034 PMT.

The addition of large densities (approximately 10^{13} atoms cm^{-3}) of O atoms and HN_3 to the flow tube produced no visible emissions and no significant increase in NO(γ) band emissions over background levels.

The time decays of O atoms were measured by movement of the sliding injector (the O atoms source) with respect to the fixed observation zone. Measurements of the O-atom decays in the absence of HN_3 yielded a value for the O-atom wall recombination rate of ≤ 3 s^{-1}. Addition of large pseudo-first-order densities of HN_3 in the range $(1-10) \times 10^{13}$ to the flow reactor did not substantially increase the O-atom temporal decay over the O-atom wall loss values. Consequently, we report the rate constant for the O + HN_3 reaction as an upper limit, $k \leq 2 \times 10^{-13}$. MacDonald and Coombe[21] have also measured a small rate constant for this reaction, giving an upper limit of $k \leq 1 \times 10^{-12}$ cm^3 s^{-1}.

2b. Kinetics of the Se + N_3 Reaction. The rate constant for the Se + N_3 reaction was determined from the time decay of Se atoms in a stream of N_3 radicals. Very dilute H_2Se mixtures were entrained at the point of the outer injector into a F atom stream and the ensuing H-atom abstraction reactions, (4) and (5), generated free Se atoms at densities $<1 \times 10^{12}$ atoms cm^3.

The Se atomic resonance line near 204 nm was used to monitor the decay of Se atoms in excess of N_3. N_3 densities were determined, as above, from the HN_3 flow rates. A response curve relating Se atom resonance fluorescence intensity to H_2Se flow rates was found to be linear over a wide range of H_2Se (hence, Se atom) concentrations. All kinetic decay curves were measured in the linear portion of the Se resonance fluorescence response

(17) Chase, M. W., et al. *JANAF Thermochemical Tables*, 3rd ed.; *J. Phys. Chem. Ref. Data* **1985**, 14.

(18) Habdas, J.; Wategaonkar, S.; Setser, D. W. *J. Phys. Chem.* **1987**, *91*, 451.
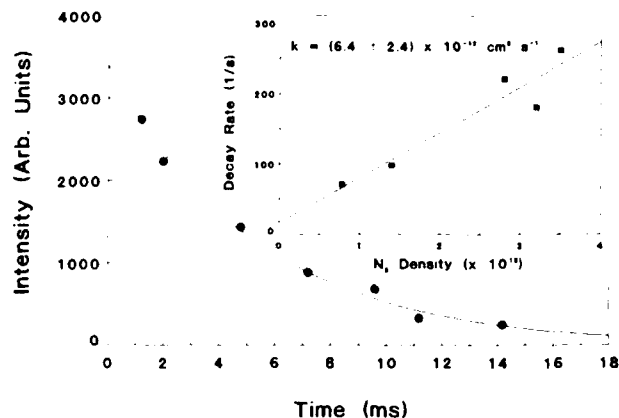
(19) Kaufman, F. *Proc. R. Soc. A* **1958**, *247*, 123.

(20) Ongstad, A. P.; Birks, J. W. *J. Chem. Phys.* **1984**, *81*(9), 3922.

(21) MacDonald, M. A.; Coombe, R. D. Unpublished result.

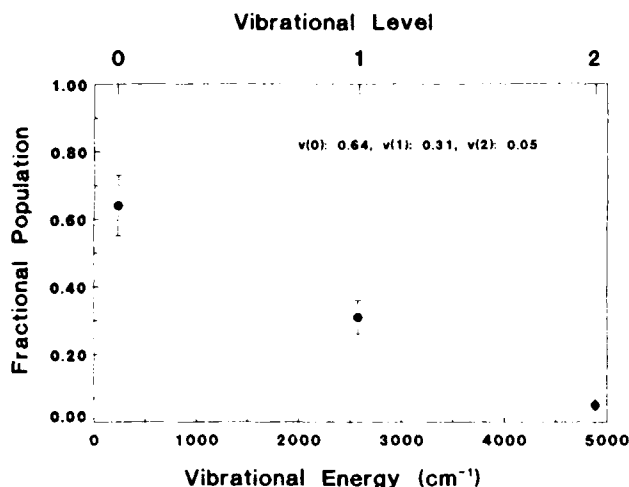**Figure 5.** Steady-state vibrational distribution in $NO(A^2\Sigma^+)$ produced by the $O + N_3$ reaction. If fit to a thermal distribution a vibrational temperature of 2594 K would be indicated.

curve. A typical decay is shown in Figure 4 and exhibits exponential behavior over several lifetimes. Figure 4 also shows a plot of the fluorescence decay rate against N_3 density. The slope of the line gives the rate coefficient for the $Se + N_3$ reaction, yielding $k = (6.4 \pm 2.4) \times 10^{-12}$ cm^3 s^{-1}. The intercept of 10 s^{-1} reveals a marginal wall loss of Se atoms on the halocarbon waxed surface.

3. NO(A) Vibrational Distribution. The radiative lifetime of NO(A) has been reported[16] to be 215 ns out of $v' = 0$. At He pressures of 2 Torr the molecule would suffer at most two collisions during its radiative lifetime. Hence, the intensity distributions from the NO spectrum should accurately reflect the nascent vibrational distribution. The upper state vibrational populations were determined from the corrected emission intensities (Figure 1) and the known Franck–Condon factors.[22]

The distribution is plotted as the fractional population of the v level against the vibration energy. From Figure 5 it is apparent that the distribution is nonthermal. As expected, no change in the distribution occurred when the bath gas pressure was varied in the 0.7–2 Torr range. The high-energy cutoff at $v' = 2$ serves to place bounds on the heat of formation of N_3 indicating: 107.8 $> \Delta H_f(N_3) \geq 101.3$ kcal mol^{-1}. The lower boundary value is close to that reported by Clark and Clyne[4] who determined $\Delta H_f = 99.15 \pm 2.3$ kcal mol^{-1}. The values reported by Habdas et al.[18] and by Pellerite et al.[23] are above the upper limit. The data indicates that 21% of the excess energy is channeled into vibration.

As a check on the experimentally determined vibrational populations and to obtain information on rotational temperatures, a computer code[24] was employed which fitted synthetic to experimental spectra. The calculation used the following equation to give the photon count $(I_{v'j''}^{v''})$ for a vibration–rotation line in spontaneous emission

$$I_{v'j''}^{v''} = \frac{64\pi^4 B_{v'} S_{J'J''}}{3hkT_r} \exp\left[\frac{-B_{v'}J'(J'+1)}{kT_r}\right] \bar{\nu}^3 x \langle v'|R_e|v''\rangle N_{v'}$$

where $B_{v'}$ is the vibration level dependent rotation constant, $S_{J'J''}$ is the Honl–London factor, T_r is the rotational temperature, $\bar{\nu}^3$ is the frequency, R_e is the electronic transition moment, and $N_{v'}$ is the population in level v'. Since the Born–Oppenheimer approximation is applied in the calculation of the experimentally determined $N_{v'}$ the transition moment integral takes the form $\langle v'|R_e|v''\rangle = R_e^2\langle v'|v''\rangle$. The fit of the synthetic to experimental spectrum, shown in Figure 1, supports the overall experimental $N_{v'}$ determination. From analysis of line widths, the fit also

(22) Jain, D. C.; Sahni, R. C. *Trans. Faraday Soc.* **1981**, *64*, 3169.
(23) Pellerite, M. J.; Jackson, R. L.; Brauman, J. I. *J. Phys. Chem.* **1981**, *85*, 1624.
(24) Lawconnell, R. I. "NS(B) Spectrum Theory and Code"; FJSRL TR-89-0005; USAFA CO 80840, 1989.

indicates a rotational temperature of 1800 ± 600 K.

4. Quantum Yield of NO(A) and NSe(A). The yield of NO(A) and NSe(A) photons produced in the $O/F/HN_3$ and $F/H_2Se/HN_3$ systems, respectively, were determined by a procedure identical to one used previously.[6] In brief, the air afterglow reaction (10)[25] is utilized to determine a calibration factor α, which is a measure of the light collection efficiency of the detection system. The calibration factor may then be applied to measurements of the NO(A) or NSe(A) emission intensity. The photon flow is then determined from the volume integrated observed intensity as

$$\text{photon flow} = \int\int I_{\text{obsd}}(\lambda,v)\, d\lambda\, dv/\gamma'\alpha$$

where γ' is the fraction of $NO(A\rightarrow X)$ or $NSe(A\rightarrow X)$ photons detected.

The yield is then given by

$$\phi = \frac{\text{photon flow}}{[N_3]} \times 100$$

where N_3 is the limiting reagent and is calculated assuming unit conversion of HN_3 to N_3 via reaction 6. Repetitive measurements of α and β were made and give $\phi_{A\rightarrow X}^{NO} = 0.3\%$ and $\phi_{A\rightarrow X}^{NSe} = 0.02\%$ with an uncertainty, characteristic of such measurements, of 50%.

Discussion

From the data, it appears that NO(A) and NSe(A) are generated by the $O + N_3$ and $Se + N_3$ reactions, respectively. In both the $O/F/HN_3$ and $H_2Se/F/HN_3$ systems, the source of the N_3 radicals is the rapid $F + HN_3$ reaction. The upper limit obtained for the rate constant of the $O + HN_3$ reaction indicates that it is a negligible source of N_3 radicals and does not influence the kinetic measurements for reaction 1.

In both systems, the observation of $NF(b\rightarrow X)$ emission in the visible region reveals that a reaction between F atoms and N_3 (7) occurs to some extent. In the $O/F/HN_3$ system, since high densities of HN_3 were used, the majority of F atoms were consumed by the $F + HN_3$ "titration reaction" (99.3% in 1 ms) and only very weak NF(b) emission was observed. However, in the $H_2Se/F/HN_3$ system F atoms were in excess of the HN_3 density and the NSe spectrum is strongly overlapped by NF(b) chemiluminescence. The importance of the $F + N_3$ reaction in this system depends upon which value of the rate coefficient for reaction 7 is used. Two widely differing values for this rate constant have been reported.[11,18] By using nitrogen first positive emission, produced by the $N + N_3$ reaction, as a tracer for N_3 radicals and by observing the change in this emission as a function of F atom density, David and Coombe[11] have determined a value of $k = (1.8 \pm 0.4) \times 10^{-12}$ cm^3 s^{-1} for reaction 7. Their measurements were made using a 3.5 cm i.d. PTFE discharge flow reactor with HN_3 (hence N_3) densities near 10^{13} molecules cm^{-3}. Habdas and co-workers[18] also employed discharge flow methods in their measurement of the rate constant, although they used a much larger flow reactor (8 cm i.d. Pyrex tube coated with halocarbon wax) and lower HN_3 densities, on the order of 7×10^{11} molecules cm^{-3}. By modeling the temporal behavior of the NF(a) chemiluminescence from reaction 7, they determined a significantly larger value of $(5 \pm 2) \times 10^{-11}$ cm^3 s^{-1} for the rate constant. For the F-atom densities employed in the $Se + N_3$ kinetic experiments, the larger value indicates that the majority of N_3 radicals would be converted to NF and N_2 (>99% conversion in 2 ms), the products of the F plus N_3 reaction. If this were indeed the case, the observation of the NSe(A) chemiluminescence could no longer be attributed to the $Se + N_3$ reaction; rather a reaction between Se atoms and NF must be hypothesized to account for the emission:

$$Se + NF \rightarrow NSe + F \qquad \Delta H_0 = -19.7 \text{ kcal mol}^{-1} \quad (12)$$

Since reaction 12 is not sufficiently energetic to populate the A

(25) Fantijn, A.; Meyer, C. B.; Schiff, H. I. *J. Chem. Phys.* **1964**, *40*(1), 64.
(26) Sloan, J. J.; Watson, D. G.; Wright, J. S. *Chem. Phys.* **1979**, *43*, 7.

state directly, either a secondary energy-transfer reaction involving nitrogen metastables or a direct reaction involving the more energetic NF(b) is required to explain the NSe(A) luminescence. The quenching experiments with NO(X), explained above, indicate energy transfer via nitrogen metastables is not the primary source of NSe* in these experiments. Further, an experiment was designed to test the role of NF(b) as an energetic reactant in the system. In this experiment, F atoms and HN₃ were introduced collinearly 43 cm upstream of the central injector (used to introduce the H₂Se into the flow reactor). The long reaction time (45 ms) and large densities of F atoms ensured completion of reaction 7 and the formation of NF(b). The green NF(b) emission was observed along the entire reaction length but diminished in intensity at longer reaction times. On adding H₂Se to the flow reactor, intense NF(b) emission was observed downstream from the central injector. The enhancement of the NF(b) flame presumably arises from the energy pooling reaction between NF(a) and HF(v) where the vibrationally excited HF is formed by reactions 4 and 5. Very little NSe(A) luminescence was detected in this experimental configuration. In fact, the emission produced here was not visible to the eye, being over an order of magnitude less intense than that observed in the previous experiments. These data support the smaller value for the F + N₃ rate constant. Similar conclusions were drawn in earlier investigations.[1b,3a,6]

If it is assumed that the NO(A) emission is produced by reaction 1, then the intensity of the γ bands can be described by the following steady-state expression
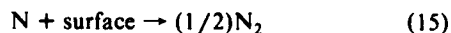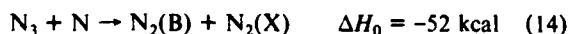
$$I_\gamma = (k_1[\text{O}][\text{N}_3])/k_r$$

where k_1 is the rate coefficient for the O + N₃ reaction and k_r is the NO(A→X) radiative rate (4.6 × 10⁶ s). Thus, the intensity varies as the product of the O and N₃ densities. Under conditions of pseudo-first-order densities of O atoms, as was employed in the present experiments, the I_γ becomes a sensitive tracer for N₃ densities and may be described by an exponential decay

$$I_\gamma \sim [\text{N}_3]_t = [\text{N}_3]_0 \exp\{(k_1^1 + k_w)t\}$$

where $[\text{N}_3]_0$ is the initial N₃ density, k_1^1 is the pseudo-first-order rate constant for the O + N₃ reaction, and k_w is the wall removal rate for N₃ radicals. Figure 3 shows a typical time profile of the NO(A) emission which has been fit to an exponential function of the form given above. The exponential fit gives the "observed decay rate" which is a sum of first-order rates: $k_1^1 + k_w$. As shown in Figure 3, the observed decays may be plotted as a function of [O] to obtain k_1 and k_w.

The wall removal processes are thought to comprise the following reactions.[11]

$$\text{N}_3 + \text{surface} \rightarrow \text{N}_2 + \text{N} \qquad \Delta H_0 = 14 \text{ kcal} \qquad (13)$$

$$\text{N}_3 + \text{N} \rightarrow \text{N}_2(\text{B}) + \text{N}_2(\text{X}) \qquad \Delta H_0 = -52 \text{ kcal} \qquad (14)$$

$$\text{N} + \text{surface} \rightarrow (1/2)\text{N}_2 \qquad (15)$$

Many studies of azide kinetics, where the F + HN₃ reaction has been used to generate N₃ radicals, report strong N₂(B→A) emission.[2a,b] In the H₂Se/HN₃/F system, where large F-atom and HN₃ flow rates were required to optimize the NSe(A) chemiluminescence, strong N₂(B→A) was indeed observed and presumably arises from the mechanism above. In contrast, no N₂(B→A) emission was observed in the O/F/HN₃ system. The N₃ wall loss mechanism indicates that the first positive intensity will vary as the product of the N and N₃ densities. Since much lower F atom flows were required to generate intense NO(A) emission for the spectral and kinetic studies, the much smaller N₃ densities in this system precluded the observation of the first positive emission. As expected, large increase in the F-atom flow rates resulted in the observation of intense NF(b) emission, the appearance of first positive, and a substantial reduction in the NO(A) intensity.

The O + N₃ reaction has been studied previously by Clark and Clyne[4] and by Piper and co-workers.[5] The former researchers noted the γ-band emission as well as an intense air afterglow when they added O atoms to a stream of chlorine azide. They attributed

the production of NO(A) to reaction 1 and the air afterglow to the subsequent recombination of O atoms with NO (reactions 10 and 11). A more detailed investigation of the reaction was performed by the latter group who utilized a unique thermal source to generate N₃ radicals. The radicals, produced in a small oven by thermally decomposing NaN₃, were mixed with small concentrations of O atoms and the resultant chemiluminescence was observed. The γ-band and air afterglow emissions observed were attributed to reaction 1 and the O + NO recombination reaction, respectively. By monitoring the intensity of the γ bands as a function of [O], they determined a rate constant for reaction 1 which is in close agreement with the value determined in this work. Further, our general observations on the γ-band emission concur with these studies. One aspect of our system which differs from the previous work is the lack of NO₂* chemiluminescence. Since reaction 1 forms NO at densities near the initial N₃ densities and since the initial O atom densities are given by the O₂ flow rates and the fractional dissociation for O₂ (near 50%) the relative amounts of NO and O atoms in the flow reactor can be estimated. These densities were near 1 × 10¹² molecules cm⁻³ and 2.5 × 10¹² atoms cm⁻³ for NO(A) intensities typical of these experiments. An experiment was performed to check the OMA sensitivity for detecting the NO₂* chemiluminescence under these conditions. All flows of gases except O₂ (i.e., O atoms) and He were removed and a flow of NO introduced. The OMA response as a function of added NO was then monitored. The air afterglow was not detectable for NO concentrations below 1 × 10¹⁴ molecules cm⁻³ which is well below the NO densities generated by the O + N₃ reaction when operated under nominal flow conditions for the O/F/HN₃ system.

The photon yields measured for the O + N₃ and Se + N₃ reactions represent the flow of NO(A→X) and NSe(A→X) photons, relative to the limiting N₃ flow, respectively. Most likely, the branching fractions reported herein are larger since collisional quenching and removal of N₃ by other processes has not been taken into account. An increase in yields of the excited diatomics NCl(a) and NF(a) has been observed in the F (or Cl) + HN₃ systems when gases normally considered collisional deactivators (e.g., CO₂ and SF₆) have been added to the flow reactors.[2] These gases are believed to act as stabilizers of the fragile N₃ radical, capable of removing the internal excitation of the N₃ where the internal modes have been excited by the heat of the reaction. The yields of the excited halide diatomics have been observed to double on addition of the stabilizer.

The yield determined for the O + N₃ reaction of 0.3% is in good agreement with the value determined by Liu and Coombe[27] who also employed the O + NO reaction to calibrate the light collection efficiency of their detection system and whose definition of photon flux and yield is identical with our own. By passing dilute O₂/He mixtures through a microwave discharge to produce the requisite O atoms, they determined $\phi_{A\rightarrow X}^{NO} = 0.44\%$. To check for possible systematic errors associated with O atom source chemistry they made additional measurements using the rapid 2F + H₂O reaction to generate the O atoms. This method gave $\phi = 0.42\%$, indicating that the yield, as expected, was independent of the manner in which the O atoms were produced.

Table 1 compares the reactions of the group VI atoms with N₃ radicals. Without exception the yields in these reactions are quite low and even if doubled they clearly do not approach other R + N₃ reactions, such as the N + N₃ reaction where spin and orbital constraints have been shown to be strong. As noted above, to the extent that angular momentum constraints are operative, these reactions are driven to produce states correlating to N(²D) + R(³P), i.e., NO(B), NS(B), and NSe(A). The reactions of the heavier atoms (S and Se) do produce the expected states, although, aside from the low-lying quartet states (a ⁴Π, and B⁴Σ⁻) which are typically only observed through spectral perturbations, the NS(B²Π) and NSe(A²Π) are the only accessible states within the energy limitations of reactions 2 and 3. In contrast, the NO(B²Π) states is not allowed in the O + N₃ reaction which produces the

---

(27) Liu, X. Ph.D. Thesis, University of Denver, 1989.

TABLE I: Summary of Group VI Atom plus N_3 Reactions

reaction	ΔH (cm^{-1})		branching fraction, %		
			exptl	prior	ref
$O(^3P) + N_3 \rightarrow NO + N_2$ 1.1×10^{-11} cm^3 s^{-1}	47901	NO(A)	0.30	0.01	TW^a
$O(^1D) + N_3 \rightarrow NO + N_2$ 1.0×10^{-10} cm^3 s^{-1}	63821	NO(A)		0.24	1c
$S(^3P) + N_3 \rightarrow NS + N_2$ 3.5×10^{-11} cm^3 s^{-1}	35770	NS(B)	0.06	0.51	6
$Se(^3P) + N_3 \rightarrow NSe + N_2$ 6.4×10^{-12} cm^3 s^{-1}	27350	NSe(A)	0.02	0.54	TW

^{a} TW = this work.

$NO(A^2\Sigma^+)$ state exclusively from several energetically allowed states. These observations indicate that the orbital angular momentum constraints are not strong in the group VI reactions.

A central issue in the group VI atom plus N_3 reactions is the question of energy disposal. The low yields suggest that these reactions may distribute their exothermicities in a purely statistical fashion with no dynamical constraints. In order to evaluate this assumption a statistical model[28] was used to predict the statistical or "prior" branching fractions for the reactions. The computed statistical branching fractions, shown in Table I, are small and as such are broadly consistent with what was observed experimentally. This would support the view that there are no strong dynamical correlations in these reactions. Further, this is consistent with the orbital correlation diagram for group VI atom plus N_3 reactions[29] which indicates a large number of mixed doublet and quartet surfaces available to the $R(^3P) + N_3(X^2\Pi_g)$ reactions. However, the $O + N_3$ reaction is clearly unique among the group VI atom reactions since it does not generate the $B^2\Pi$ state (even in the more energetic $O(^1D) + N_3(X^2\Pi_g)$ reaction the β bands are not observed) and the measured yield of the A state is substantially larger than can be accounted for by the prior distribution.

(28) The statistical branching ratios were calculated by a model given by: Alexander, M. H.; Dagdigian, P. J. *J. Chem. Phys.* **1981**, *33*, 13. Equations 11 and 14 were used to estimate the "prior" branching fraction k^*/k^X:

$$k^*/k^x = \frac{g^* \sum\limits_{v_1, v_2} [E^* - (G_{v_1} + G^*_{v_2})]^{5/2}(B_{v_1}B^*_{v_2})^{-1}}{g^X \sum\limits_{v_1, v_2} [E^X - (G_{v_1} + G^X_{v_2})]^{5/2}(B_{v_1}B^X_{v_2})^{-1}}$$

where g is a statistical weight factor (multiplicity times Λ degeneracy) for the product electronic state and where E^* (taken as 8440 cm^{-1} for NO(A), 10203 cm^{-1} for NS(B), and 8299 cm^{-1} for NSe(A)) and E^X (taken as 52640 cm^{-1} for NO(X), 40709 cm^{-1} for NS(X), and 32501 cm^{-1} for NSe(X)) are the total translational, vibrational, and rotational energies of the $NR^* + N_2(X)$ and $NR(X) + N_2(X)$ product channels, respectively. G_{v_1}, $G^*_{v_2}$, and $G^X_{v_2}$ are the vibrational terms for the species $N_2(X)$, NR^*, and $NR(X)$, respectively. Similarly, B_{v_1}, $B^*_{v_2}$, and $B^X_{v_2}$ are the rotational terms for the species $N_2(X)$, NR^*, and $NR(X)$, respectively. The summation is taken over all vibrational levels for species v_1 (taken as N_2) and v_2 (taken as NR) for which the quantities in the brackets remain real. Using the known spectroscopic constants[16] for N_2, NO, NS, and NSe and the calculated values for E^* and E^X the "prior" branching fractions for reactions 1–3 were calculated and the results are shown in Table I.

(29) Applying the orbital correlation rules, as originally set forh by Schuler (Schuler, K. E. *J. Chem. Phys.* **1952**, *21*(4), 624) to the $R(^3P_g) + N_3(X^2\Pi_g)$ reactions yields a total of 12 surfaces ($3^2A' + 3^2A'', 3^4A' + 3^4A''$). In contrast, the reaction of a highly excited ^1S atom with $N_3(X^2\Pi_g)$ would be more constrained having only two surfaces ($^2A' + ^2A''$).

It may be that surface hopping among the several ON_3 potential energy surfaces allowed by the reaction is very facile such that the reaction effectively "drains" into the NO(A) state.

Since it is most likely that a large fraction of group VI reaction exothermicities are distributed to the ground state or other dark states, LIF probing of the ground-state manifold may provide further insight into the energy disposal of these reactions.

A large number of rate constants have been reported for atom–azide reactions. The lighter atoms are generally more reactive such that in a family (e.g., group V) $k_N^{3b} > k_P^{3a} > k_{As}^7$ and across a period (e.g., second period) $k_C^{1a} = k_N > k_O > k_F$.[11] Integrating the group VI data into the rate data indicates that the trends across a period are not violated since $k_P > k_S^6 > k_{Cl}^2$ and $k_{As} > k_{Se}$. The group trends apparently can be reversed, e.g., $k_S > k_O > k_{Se}$ and $k_{Cl} > k_F$, unless the larger value for k_F is correct, in which case k_O appears anomalously slow.

The $R + N_3$ and $R + HN_3$ rates may be significantly enhanced by the electronic excitation of the atomic species. For example, Table I indicates that the $O(^1D) + N_3$ rate constant[1c] is approximately an order of magnitude larger than the $O(^3P) + N_3$ rate constant. An even larger enhancement occurs for the reaction of O atoms with HN_3 where $k(O^1D)/k(O^3P) > 1 \times 10^3$. If it is assumed that the E_a for the $O(^1D)$ reactions are near 0 and a reasonable increase in the Arrhenius A factor occurs when O atoms are excited to the ^1D state (i.e., $A^*/A = 15$, as is found in other $O(^1D)$, $O(^3P)$ reactions),[30] then the E_a may be estimated from the following simple expression

$$E_a = RT \ln [(A/A^*)(k^*/k)]$$

where E_a is the energy of activation for the reaction with $O(^3P)$ atoms. Substituting the measured rate constant values into the above equation gives $E_a(O+N_3) = 243$ cal and $E_a(O+HN_3) > 2500$ cal, indicating a negligible barrier in reaction 1 and a significant barrier in reaction 9.

Summary and Conclusions

The reactions of ground-state O and Se atoms with N_3 radicals have been shown to produce electronically excited $NO(A^2\Sigma^+)$ and $NSe(A^2\Pi)$ which subsequently emit in the 200–340-nm region (γ bands) and in the 345–525-nm region, respectively. The rate constants for the $O + N_3$ and $Se + N_3$ reactions were determined to be $(1.15 \pm 0.18) \times 10^{-11}$ and $(6.4 \pm 2.4) \times 10^{-12}$ cm^3 s^{-1}, respectively. A nonthermal vibrational distribution in NO(A) is generated by the $O + N_3$ reaction. Excellent agreement between experimental and synthetic NO(A→X) spectra is obtained by using the experimentally determined $N_{v'}$ in the computer code. A NO(A) rotational temperature of 1800 ± 600 K was determined by line-width analysis using the spectral simulation code.

The small yields of NO(A) and NSe(A) are interpreted in terms of the many surfaces available to the $R(^3P) + N_3(X^2\Pi_g)$ reactants, weak orbital angular momentum constraints, and the potential for disposing a large fraction of the reactant exothermicity to ground-state products. In contrast, the high yield of $N_2(B)$ ($\phi \geq 20\%$) in the $N(^4S) + N_3(X^2\Pi_g)$ reaction is attributed to the strength of the angular momentum constraints in that system.

(30) DeMore, W. B., et al. "Chemical Kinetics and Photochemical Data for Use in Stratospheric Modelling"; NASA Panel for Data Evaluations; Evaluation no. 8; JPL Publication 87-41, Pasadena CA, 1985.